3

A Passive All-optical Diode from Nonlinear Absorbers

3.1 Concept of an all-optical diode

In electronics, a *diode* is a device that allows the flow of current or charge carriers in one direction and restricts the flow in the other direction. In photonics, a structure that allows a similar non-reciprocal transmission of an optical signal is named as an *optical diode*. If transmission is obtained in a specific input direction and opacity in the opposite direction without the aid of any external agent, the device acts as an all-optical diode. In the ideal case, the diode transmission is 100% in the forward direction and it vanishes in the opposite direction, giving unitary contrast. Here light manipulates and controls light itself. These devices are currently receiving much attention as an alternative to the conventional optical isolator, which is based on linear polarizers and a magneto-optical Faraday rotator, and also for all-optical signal processing.

The 'optical diodes' so far realized include fluorescent dyes with a concentration gradient, where the competing effects of self-absorption and stimulated emission in a fluorescent dye with a concentration gradient are utilized [Mujumdar *et al*.]; SHG with spatially varying wavevector mismatch [Trevino-Palacios, *et al*.]; photonic crystal structures [Scalora et. al, Mingaleev et. al]; and liquid-crystal hetero junctions [Hwang et al.]. In the liquid crystal hetero junctions, a hetero photonic band gap structure consisting of an anisotropic nematic liquid crystal layer sandwiched between two cholesteric liquid-crystal layers with different helical pitches is used to realize spatial non-reciprocal transmission of circularly polarized light at the photonic-bandgap region. From these studies it has been realized that an asymmetric nature of the refractive index

and non-linearity are the two basic conditions for the construction of all-optical diodes [Zhou, H. *et al.*].

In this background, we thought that it would be interesting to investigate the transmission of optical pulses through structures in which the longitudinal nonlinear absorption coefficient, rather than the linear or nonlinear refractive index, is varied in some fashion. The first experiment of this kind was performed by Philip [Philip, R. et.al.], while he was on a sabbatical in the group of Prof. D.V.G.N.L. Rao at the University of Massachusetts, Boston. In this thesis we report the numerical simulations and the second set of experiments, which were done at the Raman Research Institute.

One motivation for these studies is the fact that the fabrication of such a structure is much easier compared to that of a photonic crystal. It can be intuitively argued that the spatial variations in the nonlinear absorption should lead to spectacular transmission effects, the nature of which can be calculated using appropriate propagation equations. Indeed, from numerical simulations, here we show that it is possible to obtain a high contrast, passive nonreciprocal transmission from a simple structure having a single asymmetry in the nonlinear absorption coefficient. In practice, the simplest form of asymmetry would be a sharp step in the nonlinearity, which can be achieved by placing a layer of saturable absorber material adjacent to a layer of reverse saturable absorber material. Such a device works as an all-optical diode.

3.2 Saturable absorbers

When the frequency of the incident radiation is near the resonant frequency, real transitions are excited in atoms and molecules. In some situations, the near resonant interactions can be described as if the system has only two energy levels. This is because the resonant interaction between the radiatively connected energy levels are so strong that other non-resonant interactions can be neglected. Dye molecules can be approximated as two level systems when the intersystem crossing rate is small compared to the fluorescence rate. Absorptive

transitions are very strong in these systems with large oscillator strengths. Due to the redistribution of the population of the two energy levels in a collection of two-level systems, for a high-intensity beam of light there will be a reduction in the absorption from the ground state to the excited state. As photons from the incident light beam pump electrons into the upper energy level, the ground state becomes depleted. The population in the upper state undergoes spontaneous and stimulated emission of photons. As a result, the system cannot absorb the incident light as it does at lower intensities. Thus there is an intensity dependent reduction in the absorption coefficient of the two level system. This process is called 'saturable absorption' [Shen, Y. R.], [Boyd, R. W.].

The nonlinear absorption coefficient of a saturable absorber (SA) is given by [Sutherland, R. L.]

$$\alpha_{SA}(I) = \alpha_{0SA}/(1 + I/I_s) \tag{3.1}$$

where α_{0SA} is the linear absorption coefficient, I is the intensity within the medium, and I_s is the saturation intensity (incident intensity where the absorption drops to half its original value). The corresponding propagation equation can be written as

$$\frac{dI}{dz'} = -\left(\frac{\alpha_{0SA}}{1 + I/I_s} \right) I \tag{3.2}$$

where z' is the position co-ordinate along the axis of propagation in the medium (of length L), and I is I(z', t). Equation 3.2 can be solved to give the transmission of a two level saturable absorber at steady state, in the homogeneously broadened case, as

$$T = \exp(-\alpha_{0SA} L)\exp\left(\left(I_{in}/I^{\Delta}_{s} \right)(1-T) \right) \tag{3.3}$$

where $I_s^{\Delta} = I_s\left[1+(\Delta\omega T_2)^2\right]$, with $\Delta\omega$ being the excitation frequency detuning and T_2 the phase coherence lifetime. $I_{in}(t)$ is the incident intensity at z' = 0.

3.3 Reverse saturable absorbers

If the transmission of a medium decreases at high input intensities, it is known as a reverse saturable absorber (RSA). For example, this situation can occur if the excited state absorption coefficient of a material is larger than its ground state absorption coefficient. For such an RSA based on excited state absorption, the nonlinear absorption coefficient is given by

$$\alpha_{RSA}(I) = \alpha_{0RSA} + \sigma N(I) I \tag{3.4}$$

where α_{0RSA} is the linear absorption coefficient. σ is the absorption cross section, and N(I) is the population density, of the excited state. Another cause for RSA is two-photon absorption, in which case $\sigma N(I)$ can be replaced by βI, where β is the two-photon absorption coefficient. The corresponding propagation equation is given by

$$\frac{dI}{dz'} = -(\alpha_{0RSA} + \beta I) I \tag{3.5}$$

In some cases, multiphoton absorption also can lead to RSA.

3.4 Structures exhibiting axially asymmetric nonlinear absorption

A saturable absorber or a reverse-saturable/two-photon absorber, when taken alone, shows spatially reciprocal linear and nonlinear transmission. That is, the transmission remains the same irrespective of the direction in which the light is passing through the material. Some materials are capable of showing either saturable absorption or reverse-saturable/two-photon absorption depending on the input intensity. Such materials also will show spatially reciprocal linear and nonlinear transmission of the incident laser light. But if we use a saturable absorber in combination with another material whose linear absorption reduces the

input intensity below that of the saturation intensity of the saturable absorber, then the resultant nonlinear transmission will be nonreciprocal. Therefore it logically follows that if a saturable absorber and a reverse-saturable/two-photon absorber are placed in tandem the above effect should become enhanced. The linear transmission will remain spatially reciprocal but the nonlinear transmission will become spatially non-reciprocal at those intensities where the non-linearities of the saturable absorber and the reverse saturable/two photon absorber become strong enough.

Here we consider two configurations of the nonlinear absorbers. If the SA is placed first followed by the RSA, we call it 'forward bias'. If the RSA is placed first followed by the SA, it is called 'reverse bias'. In the forward bias configuration, the input light induces a high transmittance in the saturable absorber, and the transmitted intensity will then be subsequently reduced by the reverse saturable absorber. The linear transmittance of the saturable absorber is usually low so that only when the input intensity is sufficiently high, the saturable absorber starts transmitting light appreciably. The region of linear transmission can be taken to be analogous to the knee voltage region of a forward-biased electronic diode. Once the forward bias voltage exceeds the knee voltage, current starts to flow through the electronic diode. In a similar fashion, when the intensity of the input light is sufficiently high to introduce saturation, the configuration allows light flow in that direction. In the reverse biased configuration, the intensity of the light transmitted by the reverse saturable absorber usually falls below the intensity required to evoke a high transmittance in the saturable absorber. Hence the system will give only a transmittance that is equal to or less than the linear transmittance of the combination. Obviously, the device will work in the reverse bias configuration only if the non-linear absorption coefficient of the reverse saturable absorber is such that, it brings the transmitted intensity below the saturation intensity of the saturable absorber. Because of the dynamic nature of the SA and RSA phenomena, the device will act as an optical diode only for certain appropriate combinations of the input intensity and non-linear absorption coefficients of the materials put in tandem to form the optical diode. Moreover

there will be a wavelength dependence for the all-optical diode effect because the same material can act either as a saturable absorber or a reverse saturable absorber, depending on the excitation wavelength.

To investigate the feasibility of this idea, we simulated the optical transmission of a nonlinear absorber composed of a saturable absorber and a two-photon absorber placed in tandem. In our simulation, I_s and β (Saturation intensity and TPA coefficient respectively) are taken as the nonlinear parameters. I_s values are kept in the range of 10^6 to 10^{14} W/m^2 and β values in the range of 10^{-14} to 10^{-6} m/W, which match well with most practical situations. For the forward bias simulation, a temporally Gaussian laser pulse of 7 nanoseconds FWHM (full width at half maximum) and energy E_{in} is chosen. The intensity of the Gaussian pulse ($I_{in}(t)$) is then propagated through the SA, and the output intensity is calculated using eqn.3.2. This output intensity is then fed as the input of the RSA, and the output of the RSA ($I_{out}(t)$) is calculated using eqn.3.5. $I_{out}(t)$ is then time-integrated to calculate the output energy E_{out}, and the transmission of the device is given by E_{out}/E_{in}. This process is repeated for intensity values within the range of 10^9W/m^2 to 10^{14}W/m^2 (which can be achieved in practice from a focused Nd:YAG laser). The same procedure is adopted for the reverse bias simulation, except that in this case eqn.3.5 is solved first, which is then followed by eqn.3.2.

3.5 Nonlinear transmission in an axially asymmetric nonlinear structure

Results obtained for representative values of non-linear absorption coefficient and saturation intensity are given in the figures that follow. All the transmittances are normalized to the linear transmittance of the combination of the SA and the RSA. Filled squares represent the normalized transmittance in the forward biased configuration, and filled circles represent the normalized transmittance in the reverse biased configuration. In figures 3.1 to 3.5, materials with a fixed β value are considered. The linear transmittance of the SA and RSA are systematically varied between 0.0001 and 0.75. For a given β value and linear transmittance, the I_{sat} values are changed. For figures 3.1 to 3.5 the β value is

fixed at $1x10^{-10}$ m/W, and the saturation intensity I_{sat} is varied from $1x10^{6}$ W/m^2 to $1x10^{14}$ W/m^2 with one order of magnitude increase from left to right, starting from the top left figure. Going from figure 3.1 to 3.5 it is seen that as the linear transmittance of the SA and RSA increases, the contrast of the transmission in the forward and reverse biased configurations decreases. For optimum contrast, the linear transmittance has to be chosen carefully. (The dependence on the linear transmittance of the SA is studied in detail both using simulation and experiment in sections 3.6 and 3.7 respectively.) From these figures it is clear that as the saturation intensity varies for a fixed β value and linear transmittance, the regions of input intensity where the device offers a contrast in transmission changes. For certain optimum values of I_{sat} the contrast is good and there will be a reduction in the net transmittance in the reverse bias configuration. Hence it is necessary to find out the optimum range of parameters for a given set of materials and input laser intensities.

For drawing figures 3.6 to 3.10, an I_{sat} value that gives good contrast and reduction in the reverse bias transmittance is chosen, from the simulations in figures 3.1 to 3.5. The β value then is varied for a fixed combination of the linear transmittance of SA and RSA. For figures 3.6 to 3.10, the I_{sat} value is fixed at $1x10^{12}$ W/m^2 and β is varied from $1x10^{-14}$ m/W to $1x10^{-06}$ m/W, with one order of magnitude increase from left to right starting from the top left figure. With increasing β value the reverse biasing is seen to be more effective. When the β value is very high, the nonlinear absorption at high intensities becomes so large that practically no light is transmitted in the reverse bias configuration. It is observed from figures 3.1 to 3.10 that the linear transmittance of the SA and RSA should be less than 0.1 to get a good contrast between the forward and reverse bias transmittances (nonreciprocal transmission). For instance, from figures 3.5 and 3.10 it is obvious that for a linear transmittance of 75%, the transmission is completely reciprocal.

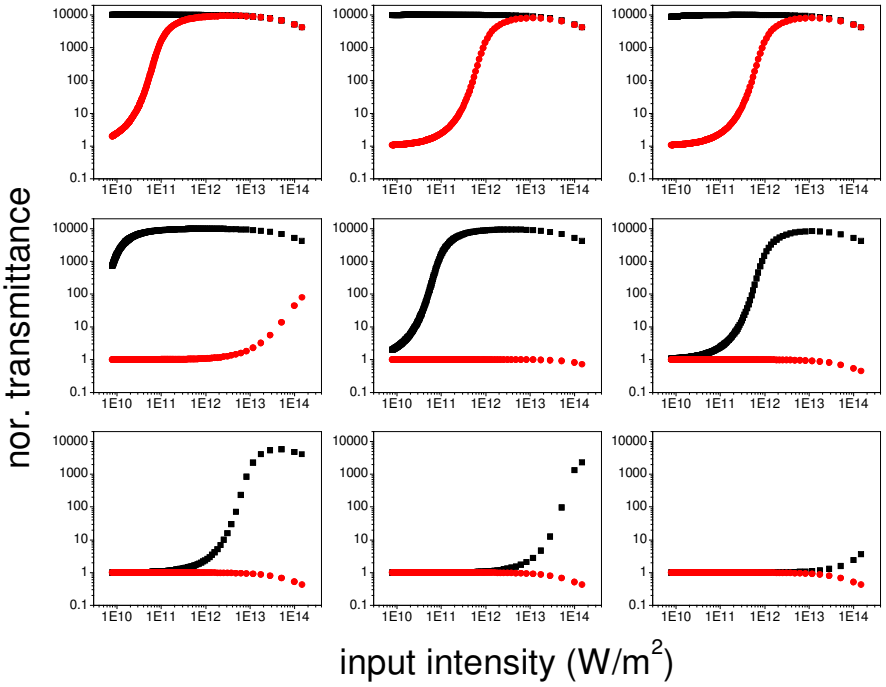

Figure 3.1: Linear transmittance of SA and RSA= 0.0001, $\beta = 1x10^{-10}$ m/W.

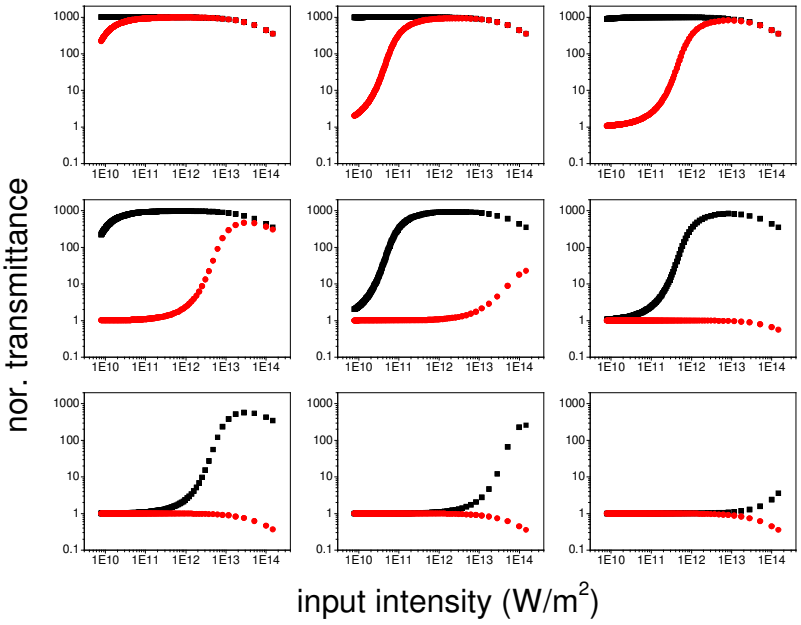

Figure 3.2: Linear transmittance of SA and RSA= 0.001, $\beta = 1x10^{-10}$ m/W.

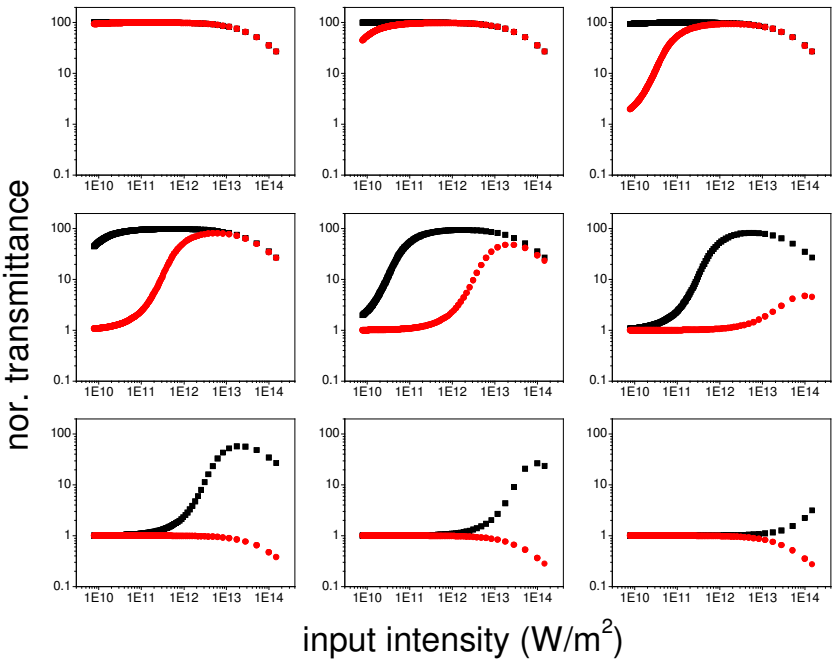

Figure 3.3: Linear transmittance of SA and RSA= 0.01, $\beta = 1x10^{-10}$ m/W.

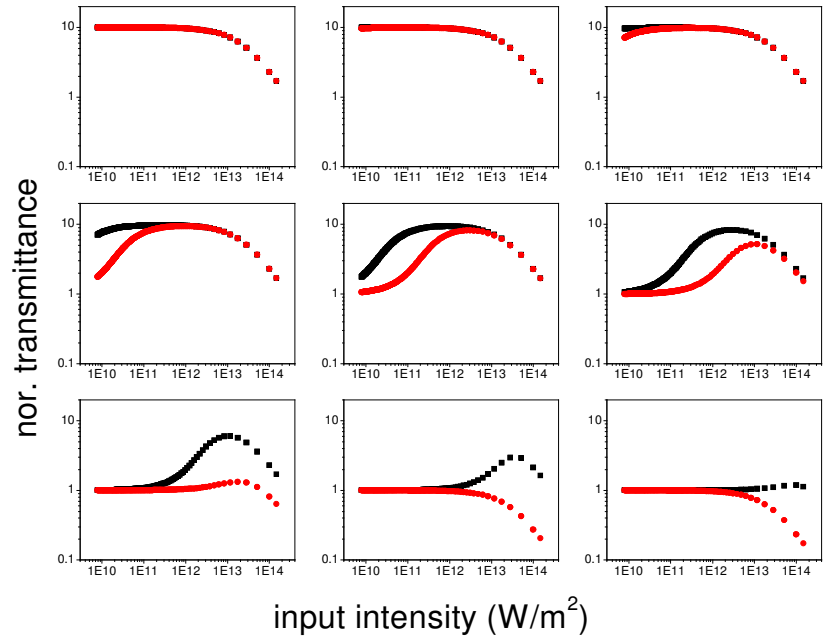

Figure 3.4: Linear transmittance of SA and RSA= 0.1, $\beta = 1x10^{-10}$ m/W.

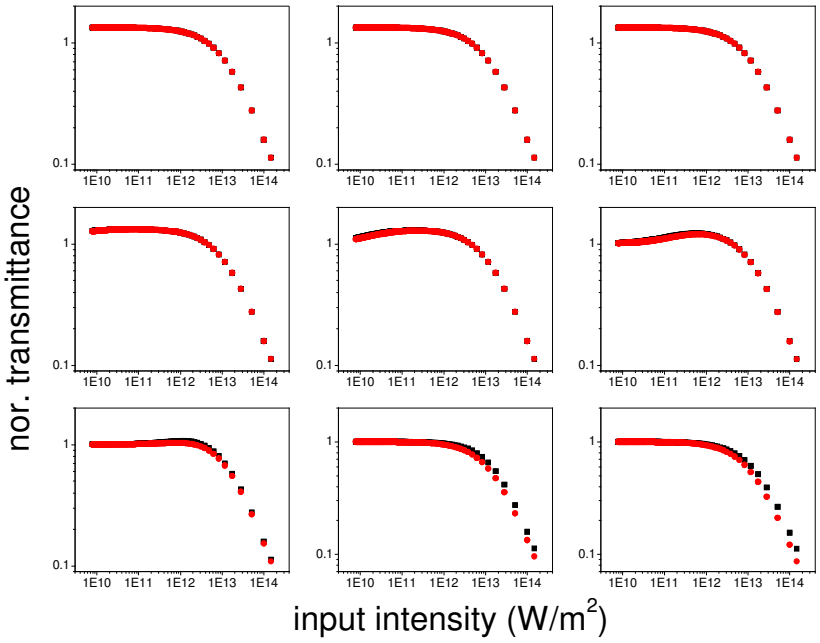

Figure 3.5: Linear transmittance of SA and RSA= 0.75, $\beta = 1x10^{-10}$ m/W.

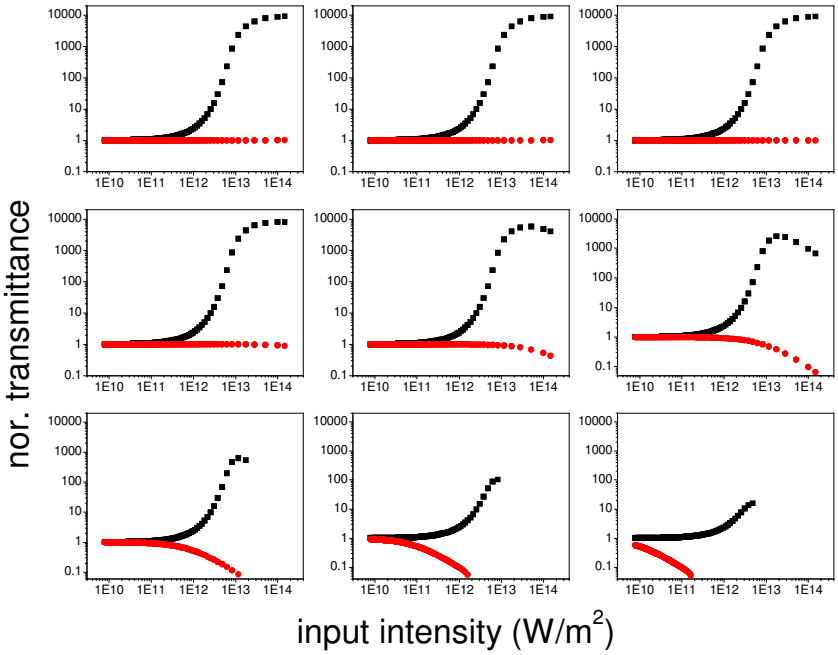

Figure 3.6: Linear transmittance of SA and RSA= 0.0001, $I_s = 1x10^{12}$ W/m^2.

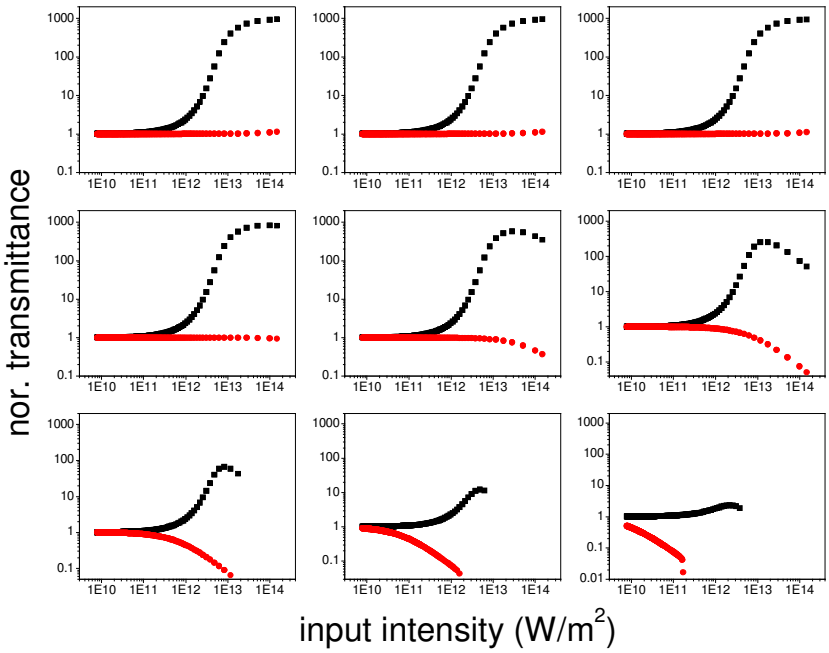

Figure 3.7: Linear transmittance of SA and RSA= 0.001, $I_s = 1x10^{12}$ W/m^2.

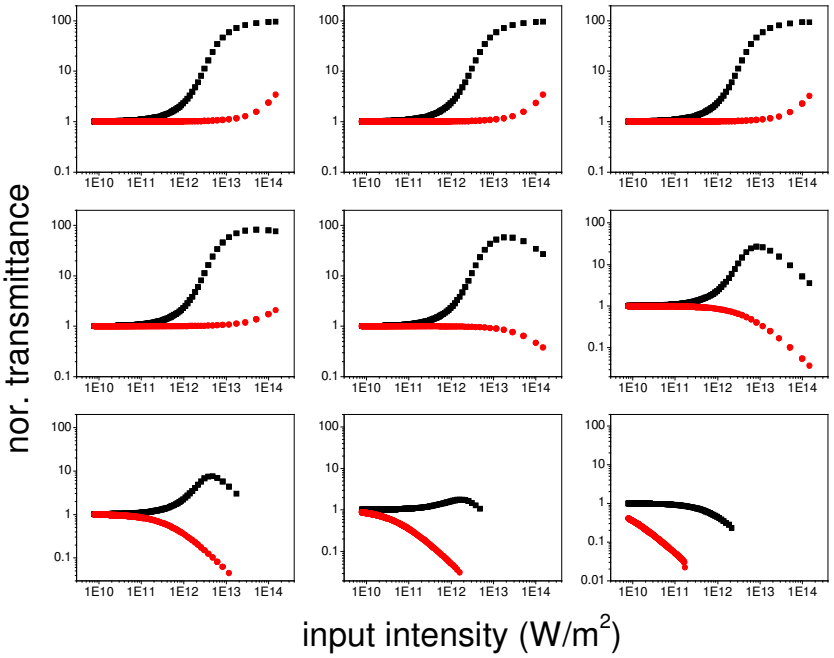

Figure 3.8: Linear transmittance of SA and RSA= 0.01, $I_s = 1x10^{12}$ W/m^2.

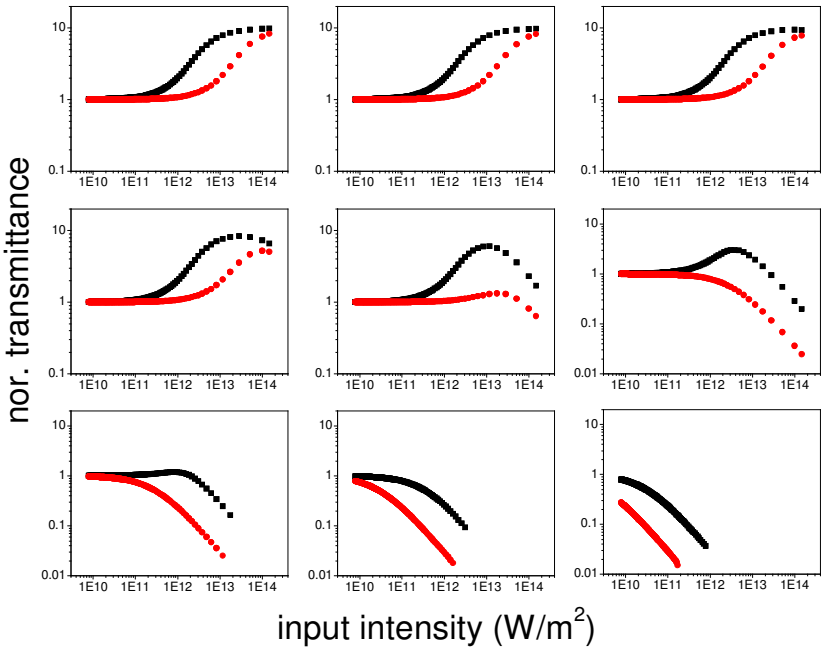

Figure 3.9: Linear transmittance of SA and RSA= 0.1, $I_s = 1x10^{12}$ W/m^2.

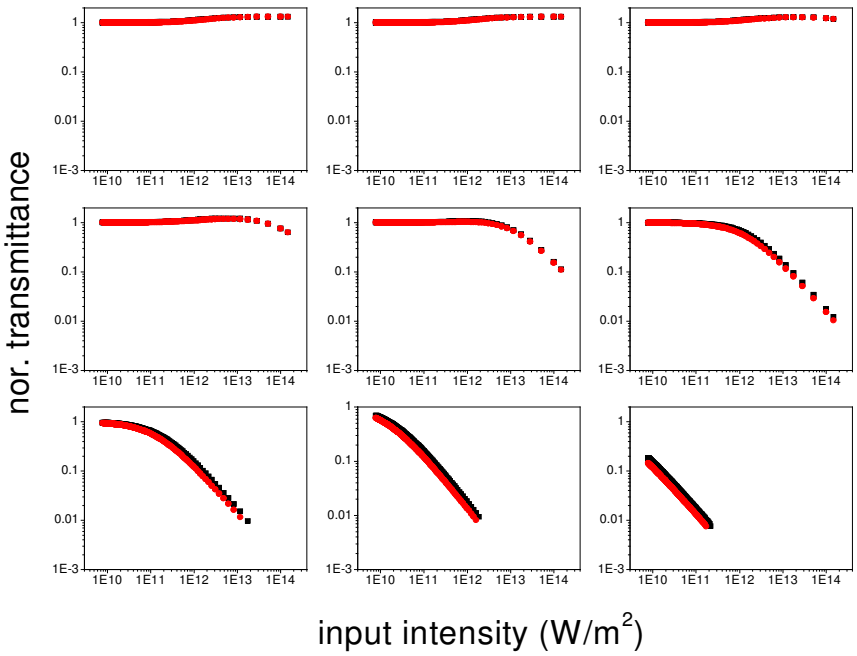

Figure 3.10: Linear transmittance of SA and RSA= 0.75, $I_s = 1x10^{12}$ W/m^2.

3.6 Effect of linear transmittance

We did more simulations to check the influence of the linear transmittance of the SA and RSA on the contrast obtained between the forward and reverse biased configurations. By fixing the linear transmittance of the SA at the two extreme values of 0.0001 and 0.75, that of the RSA is varied between 0.0001 and 0.75. The β value and I_{sat} are fixed at 10^{-10} m/W and 10^{12} W/m^2 respectively. These values are chosen from the optimum contrast nonreciprocal transmission results from figures 3.1 to 3.10.

A direct comparison of figures 3.11 and 3.12 shows that, when the linear transmittance of the SA is low, the contrast between the forward and reverse biases becomes high. When the linear transmittance of the SA is 75%, there is practically no significant enhancement in the forward bias transmittance. The reason might be that, for such a high value of the linear transmittance, the concentration of the SA is so low that the system is saturated even at low

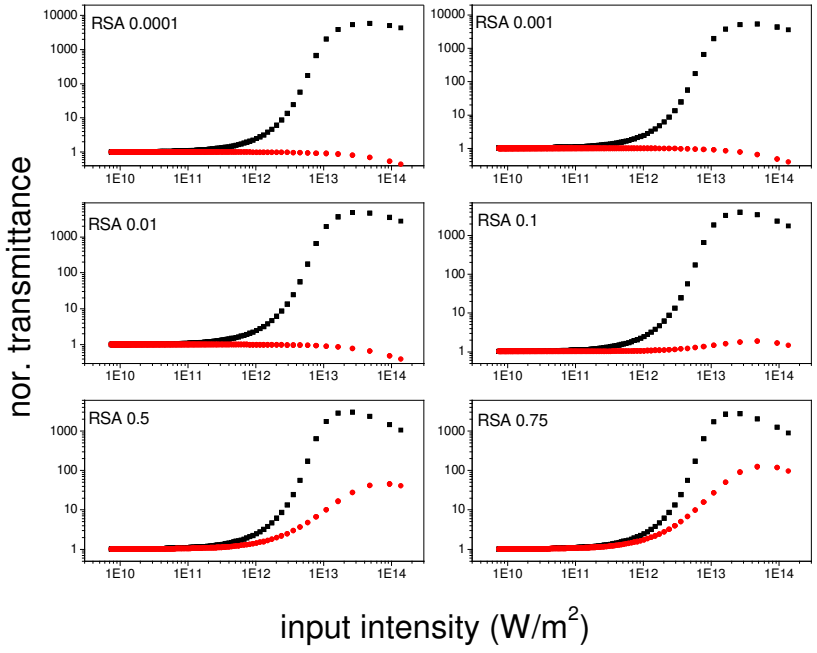

Figure 3.11: Linear transmittance of SA fixed at 0.0001.

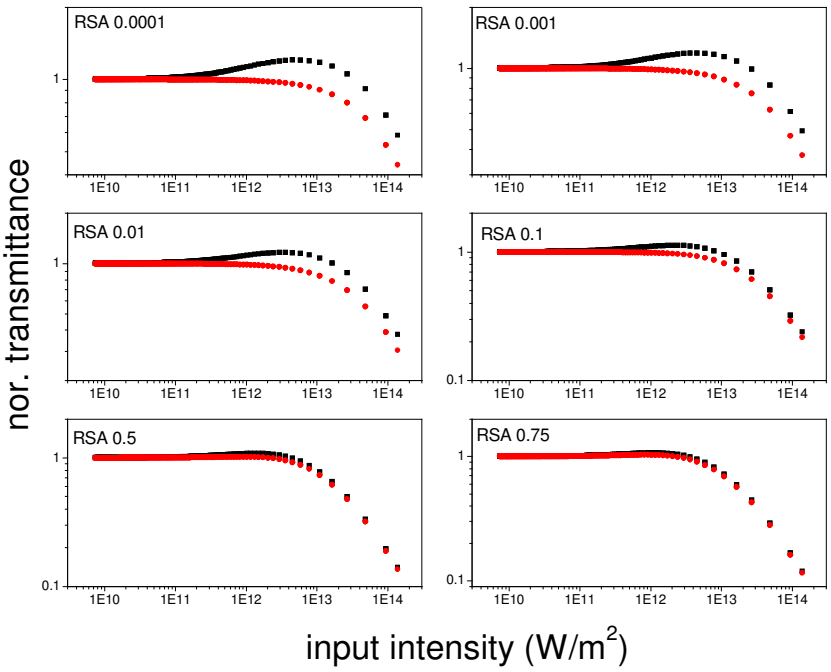

Figure 3.12: Linear transmittance of SA fixed at 0.75.

intensities. From figure 3.11 it is clear that, as the linear transmittance of the RSA is increased, the reverse bias transmittance increases reducing the contrast of the non-reciprocal action.

In figures 3.13 and 3.14, the linear transmittance of RSA is fixed at the extreme values of 0.0001 and 0.75 respectively, and that of SA is varied between 0.0001 and 0.75. Similar to figures 3.11 and 3.12, β and I_{sat} values are fixed at 10^{-10} m/W and 10^{12} W/m^2 respectively. It is seen from figure 3.13 that as the linear transmission of the SA is increased, the contrast falls drastically. More specifically, the enhancement in the forward biased transmission is substantially reduced. Thus at higher intensities the non-reciprocity is hardly retained. It is evident that in order to have a good spatial non-reciprocity at high input laser intensities, the linear transmittance of the SA should be sufficiently small.

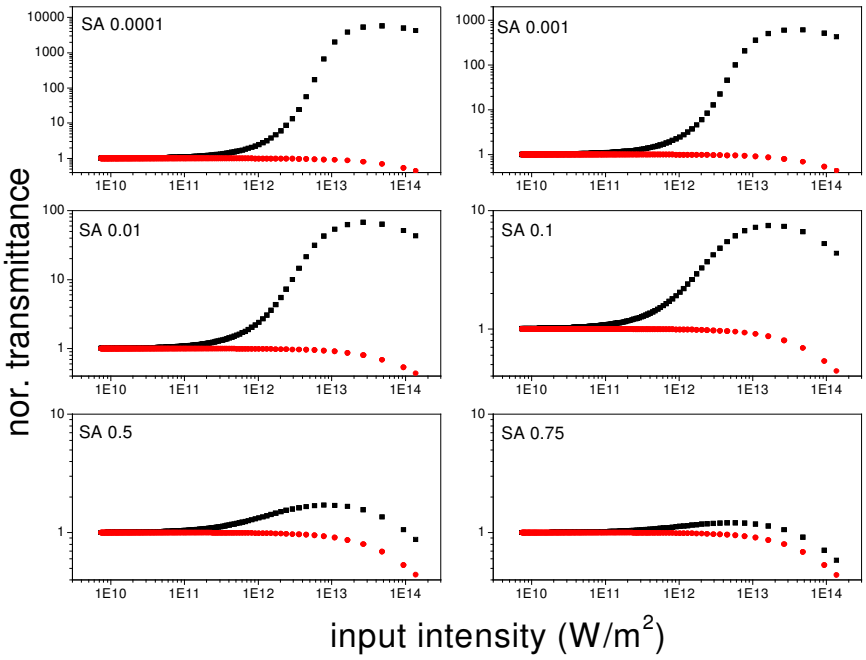

Figure 3.13: Linear transmittance of RSA fixed at 0.0001.

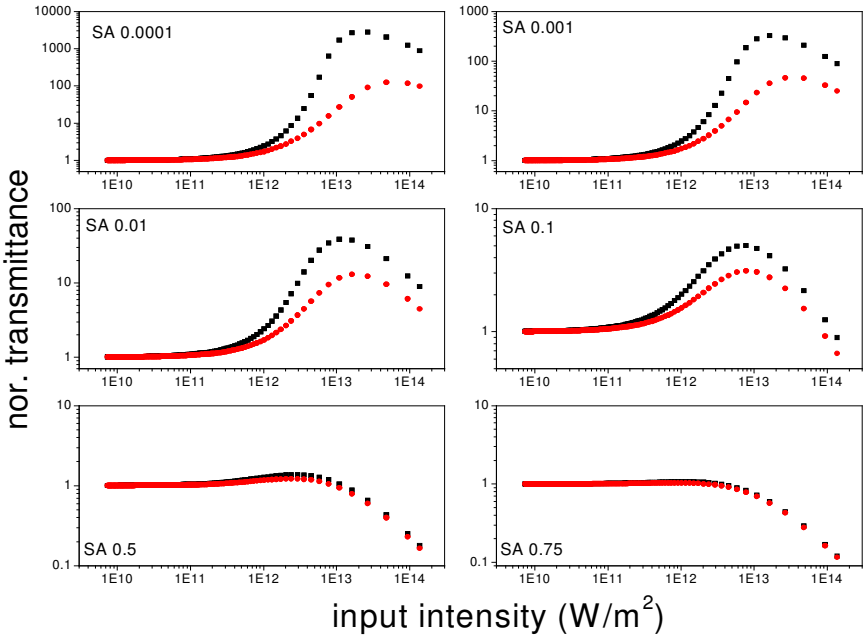

Figure 3.14: Linear transmittance of RSA fixed at 0.75.

From figure 3.14 it is clear that as the linear transmittance of RSA is increased the reverse bias transmittance behaves similar to that of forward bias. This is because, as the linear transmittance of RSA is increased more intensity reaches the SA facilitating enhancement of the transmission, unlike that of figure 3.13. Thus it is clear that, in order to get a good non-reciprocal transmission with a good contrast, the linear transmittance of the SA should be sufficiently small and that of RSA should be moderately small.

3.7 Experimental results

To confirm the simulated results we did experiments in which the laser dyes Rhodamine 6G (R6G) and Pyrromethene were used as saturable absorbers and C_{60} and LDS867 as reverse saturable absorbers. The linear transmittance of the SA and RSA are chosen such that the net transmission can be detected sufficiently above the detector noise limit. Pyroelectric detectors are used for the

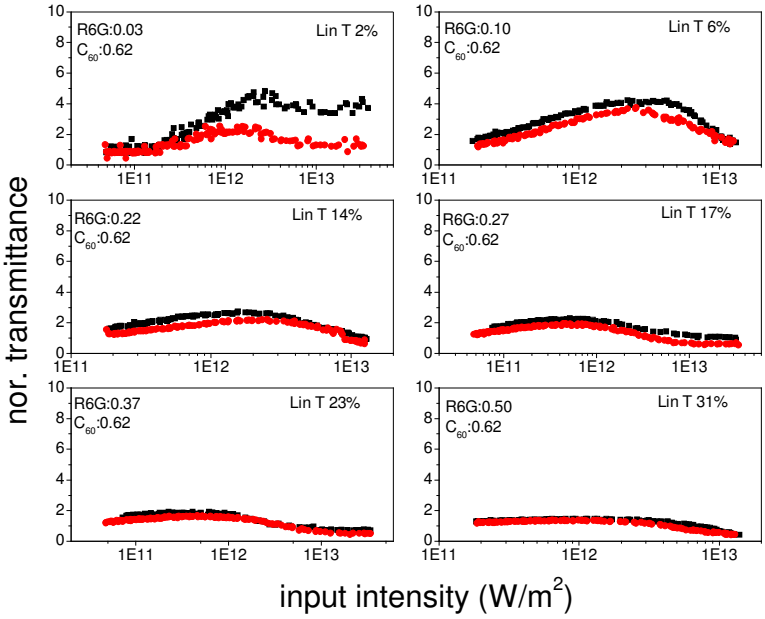

Figure 3.15: Rhodamine 6G as a saturable absorber and C_{60} as a reverse saturable absorber.

measurements. The SA and RSA placed in tandem is excited with 7ns laser pulses at 532nm. There is 550μJ of energy in each pulse, which is focused using a planoconvex lens of focal length 50cm. For doing four sets of the experiments, the linear transmission of the saturable absorbers, i.e., R6G and Pyrromethene, are varied. The linear transmittance of R6G and Pyrromethene start from a value near 0.1, which is then increased as we go from left to right and top to bottom in figures 3.15 to 3.18. It is seen that the contrast is maximum when the linear transmittance of the SA and RSA are minimum. As the linear transmittance is increased, the contrast drops in agreement with the simulation results. Even though the contrast achieved is quite low, the spatial nonreciprocal transmission is unmistakably demonstrated.

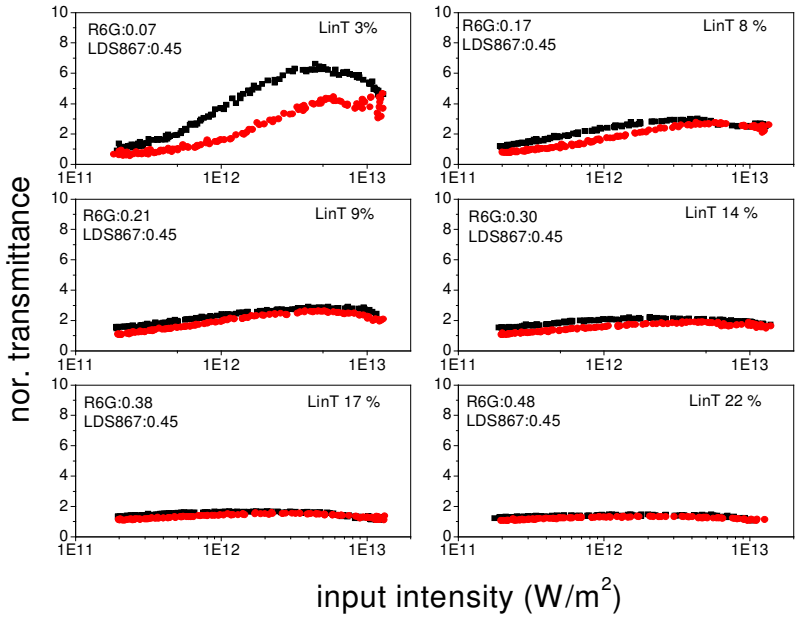

Figure 3.16: Rhodamine 6G as a saturable absorber and LDS867 as a reverse saturable absorber.

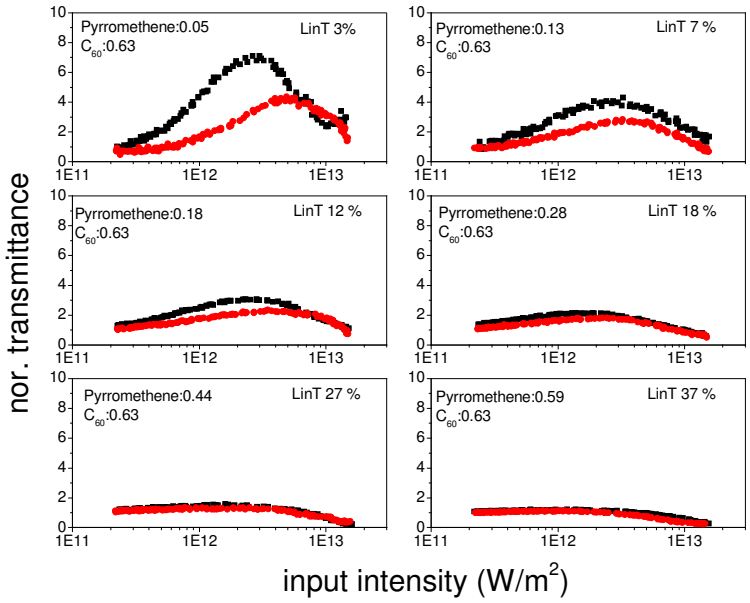

Figure 3.17: Pyrromethene as a saturable absorber and C_{60} as a reverse saturable absorber.

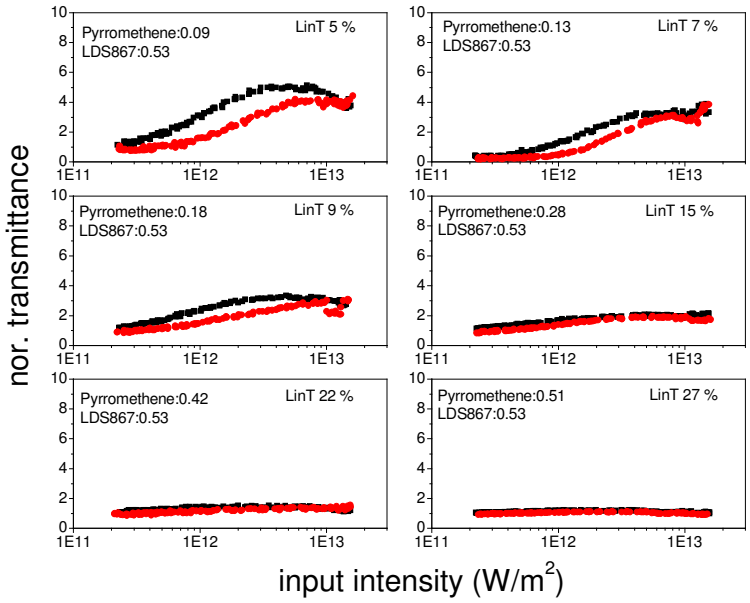

Figure 3.18: Pyrromethene as a saturable absorber and LDS 867 as a reverse saturable absorber.

3.8 Thin nonlinear media

In the previous section we demonstrated the spatial nonreciprocity of transmission using 1mm thick samples (both SA and RSA are of 1mm path length). From a device point of view it is useful to see whether the same principles will work at a thickness scale of a few micrometers. In this section this possibility is studied using simulations. If it is possible to devise a single nonlinear unit of, say, total 2μm path length with the proper I_s and β values, then that will suffice as a miniature all-optica passive diode. Depending on the wavelength of interest the appropriate materials can be selected. As a possible suggestion for practical implementation in photonic circuits, one can coat one end of a wave-guide with a very thin layer of an SA and then join it to the end of another wave-guide with a thin layer of an RSA. The junction will be acting like the depletion layer of an ordinary p-n junction diode. In figures 3.19 to 3.23 the β value is fixed at $1x10^{-10}$ m/W and the saturation intensity I_{sat} is varied from $1x10^{6}$ W/m^2 to $1x10^{14}$ W/m^2 with one order of magnitude increase from left to right starting from the top left, similar to the figures 3.1 to 3.5 for the 1mm thick samples. Linear transmittance of SA and RSA are varied from 0.0001 to 0.75. The nature of the graphs is similar to that obtained for 1mm samples. In figures 3.24 to 3.28 I_{sat} is fixed at $1x10^{12}$ W/m^2 and the nonlinear absorption coefficient β is varied from $1x10^{-14}$ m/W to $1x10^{-06}$ m/W with one order of magnitude increase from left to right starting from the top left figure. The characteristics of the graphs remain the same here too.

Thus under the thin sample approximation also, spatial non-reciprocity can be observed for the right set of nonlinear parameters. Obviously, practical implementation depends on the availability of materials with the right values of β and I_{sat} at the smaller thickness.

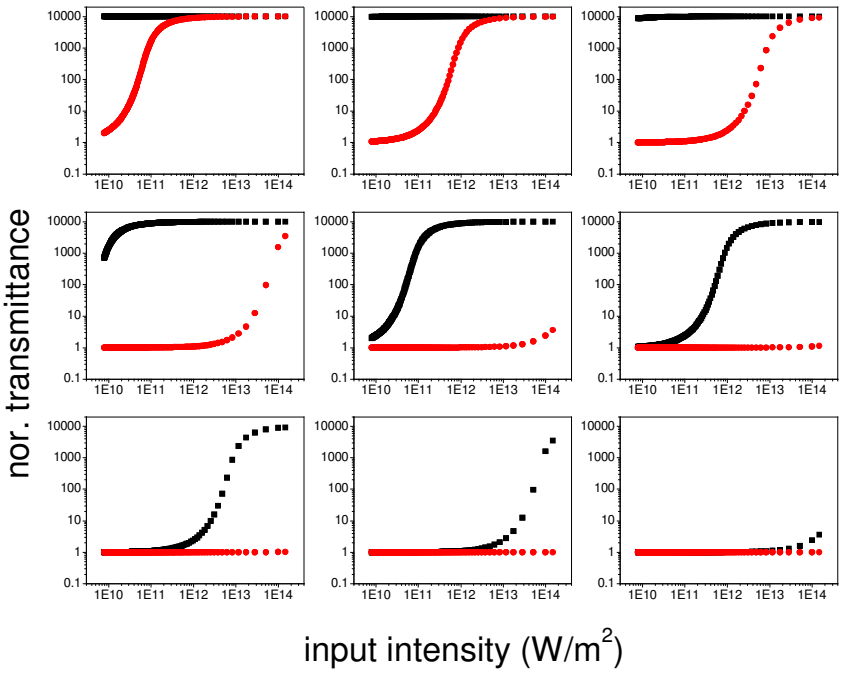

Figure 3.19: Linear transmittance of SA and RSA = 0.0001.

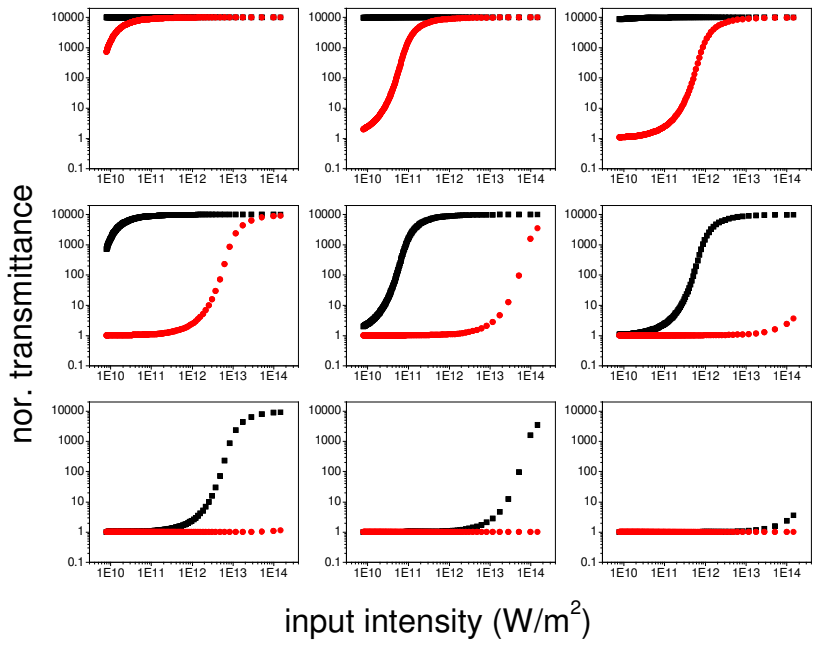

Figure 3.20: Linear transmittance of SA= 0.0001 and RSA= 0.001.

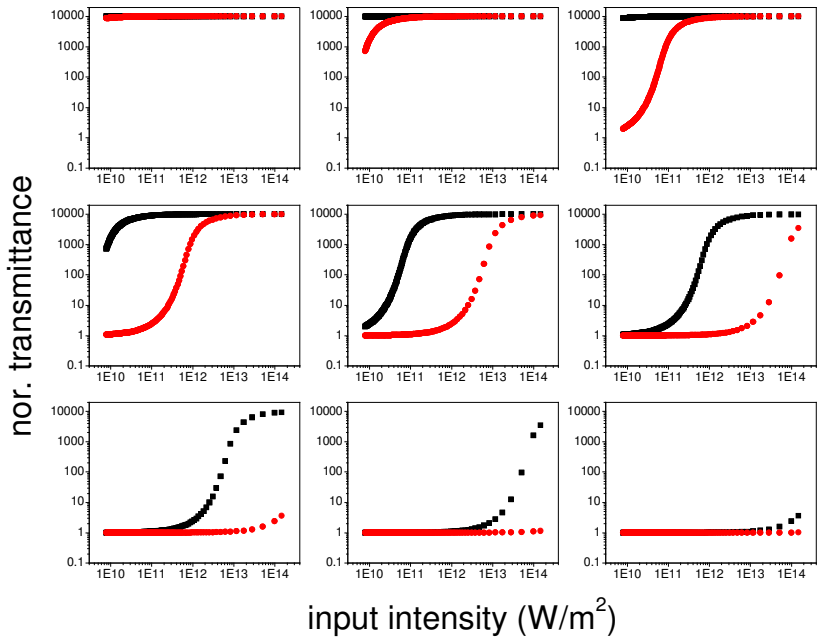

Figure 3.21: Linear transmittance of SA= 0.0001 and RSA= 0.01.

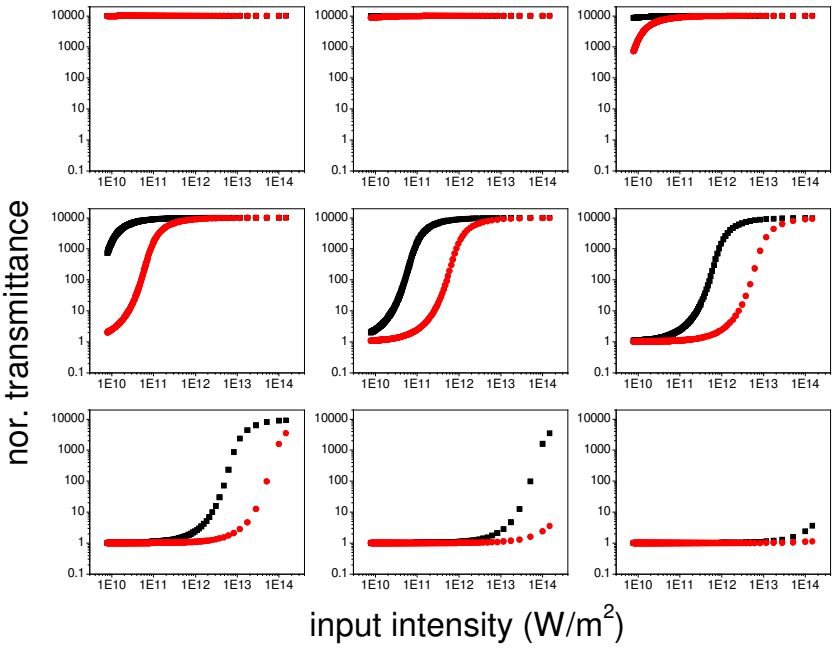

Figure 3.22: Linear transmittance of SA= 0.0001 and RSA= 0.1.

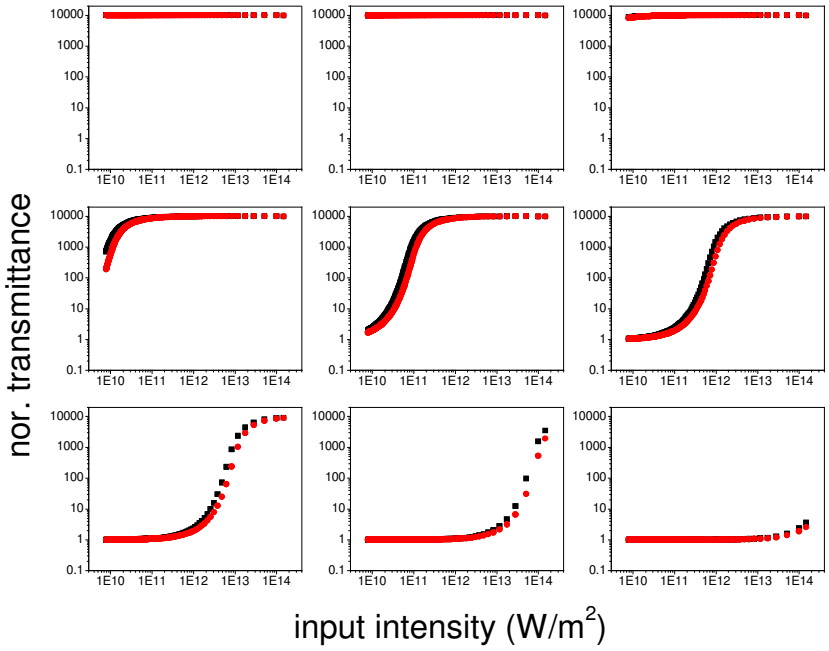

Figure 3.23: Linear transmittance of SA= 0.0001 and RSA= 0.75.

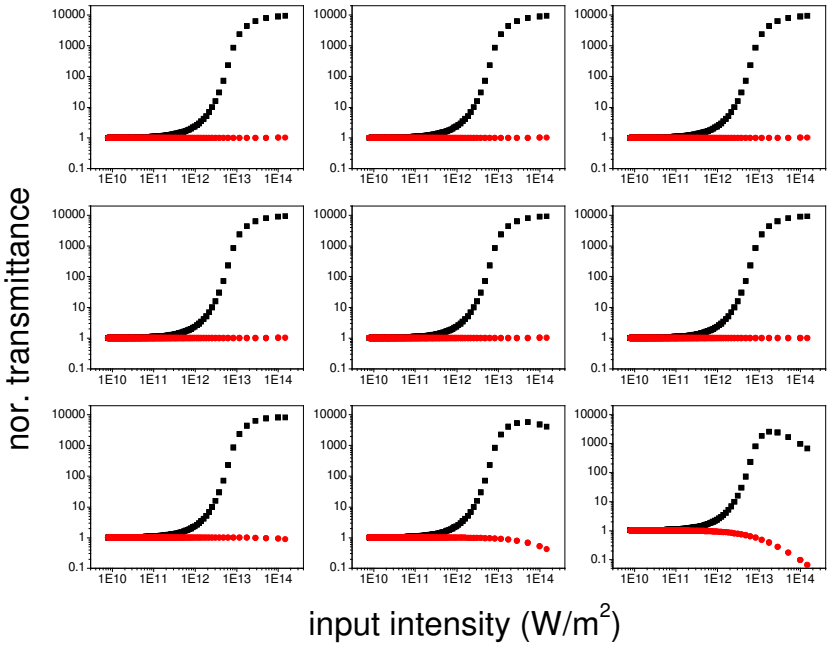

Figure 3.24: Linear transmittance of SA= 0.0001 and RSA= 0.0001.

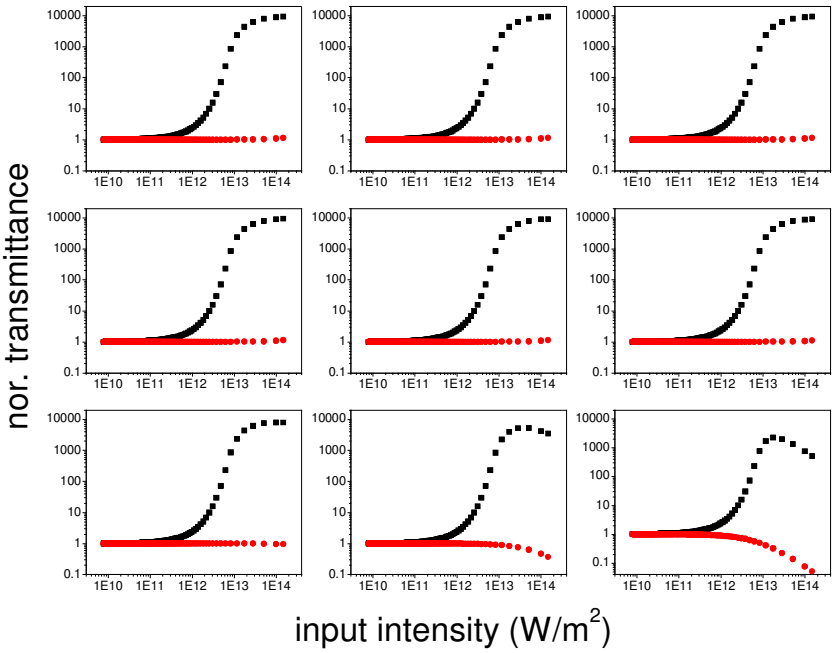

Figure 3.25: Linear transmittance of SA= 0.0001 and RSA= 0.001.

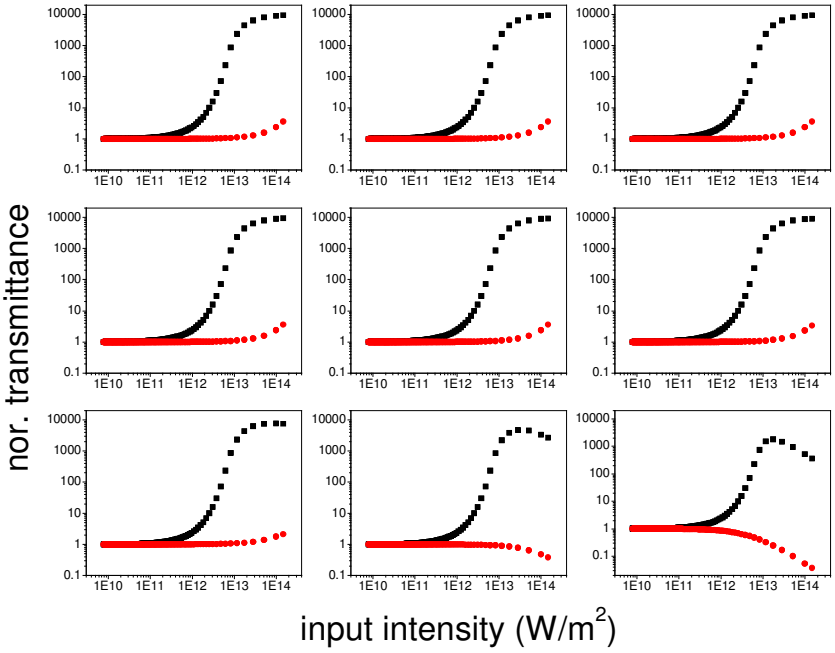

Figure 3.26: Linear transmittance of SA= 0.0001 and RSA= 0.01.

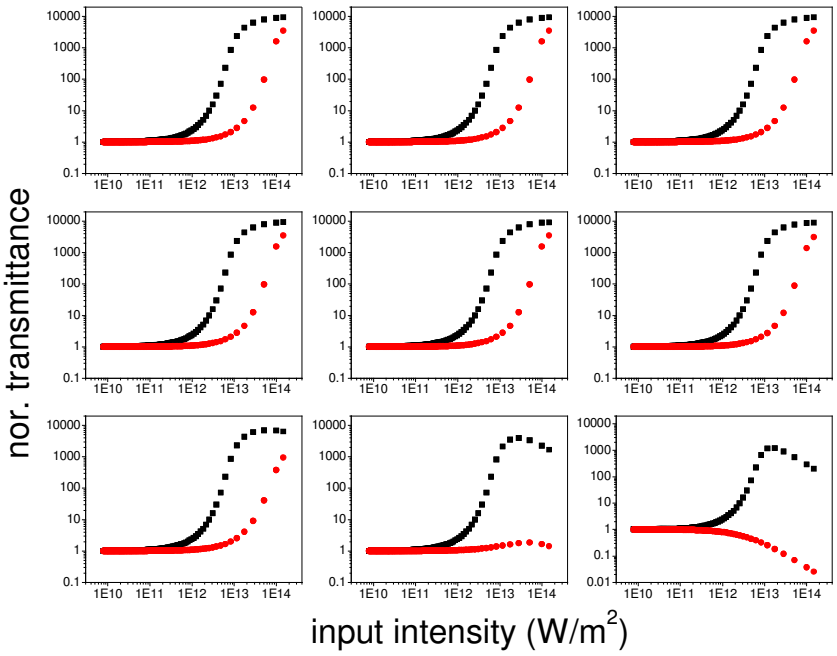

Figure 3.27: Linear transmittance of SA= 0.0001 and RSA= 0.1.

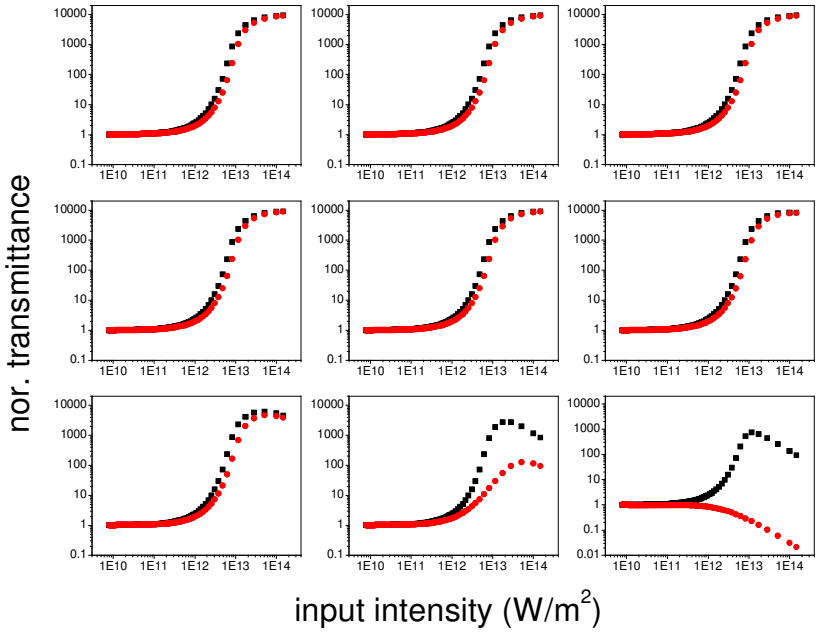

Figure 3.28: Linear transmittance of SA= 0.0001 and RSA= 0.75.

3.9 Conclusions

In this chapter the basic behavior of a structure exhibiting axially asymmetric nonlinear absorption is worked out, employing saturable and reverse saturable absorption materials in tandem. Detailed numerical simulations demonstrate all-optical diode behavior, and the results are verified experimentally. The principle will work for all light polarizations, has no phase-matching restrictions, and can be extended to a large number of available nonlinear media for possible applications. While fabrication of photonic crystals proposed for optical diode applications in the visible region are cumbersome due to dimensional constraints, the present device does not have this limitation, since the thickness of the nonlinear layers can be relatively large, in the order of millimeters. Since saturable and reverse saturable materials are available in different forms (solution, polymer films, quantum dots, metal nanoparticles etc.) for a wide range of intensities, it should be possible to develop the device as lab on a chip for waveguide and fiber optic applications.